



**HAL**  
open science

# Synthesis, characterization and optical properties of new tetrafluorenyl-porphyrins peripherally functionalized with conjugated 2-fluorenone groups

Xu Zhang, Zhipeng Sun, Nicolas Richy, Olivier Mongin, Frédéric Paul, Mireille Blanchard-desce, Christine O. Paul-Roth

## ► To cite this version:

Xu Zhang, Zhipeng Sun, Nicolas Richy, Olivier Mongin, Frédéric Paul, et al.. Synthesis, characterization and optical properties of new tetrafluorenyl-porphyrins peripherally functionalized with conjugated 2-fluorenone groups. *New Journal of Chemistry*, 2021, 45 (33), pp.15053-15062. 10.1039/d1nj01410b . hal-03245201

**HAL Id: hal-03245201**

**<https://hal.science/hal-03245201>**

Submitted on 18 Oct 2021

**HAL** is a multi-disciplinary open access archive for the deposit and dissemination of scientific research documents, whether they are published or not. The documents may come from teaching and research institutions in France or abroad, or from public or private research centers.

L'archive ouverte pluridisciplinaire **HAL**, est destinée au dépôt et à la diffusion de documents scientifiques de niveau recherche, publiés ou non, émanant des établissements d'enseignement et de recherche français ou étrangers, des laboratoires publics ou privés.

# Synthesis, Characterization and Optical Properties of New Tetrafluorenyl-Porphyrins Peripherally functionalized with Conjugated 2-Fluorenone Groups

Xu Zhang,<sup>a</sup> Zhipeng Sun,<sup>a</sup> Nicolas Richy,<sup>a</sup> Olivier Mongin,<sup>a</sup> Frédéric Paul,<sup>\*,a</sup> Mireille Blanchard-Desce,<sup>\*,b</sup> Christine O. Paul-Roth,<sup>\*,a</sup>

*Dedicated to a long-time experienced collaborator in the field of conjugated materials, Prof. Todd B. Marder, on the occasion of his 66<sup>th</sup> birthday.*

<sup>a</sup> Univ Rennes, INSA Rennes, CNRS, ISCR (Institut des Sciences Chimiques de Rennes) – UMR 6226, F-35000 Rennes, France

<sup>b</sup> Université de Bordeaux, Institut des Sciences Moléculaires (CNRS UMR 5255), 33405 Talence, France

\*Corresponding authors: [christine.paul@insa-rennes.fr](mailto:christine.paul@insa-rennes.fr) and [Frederic.paul@univ-rennes1.fr](mailto:Frederic.paul@univ-rennes1.fr) and [mireille.blanchard-desce@u-bordeaux.fr](mailto:mireille.blanchard-desce@u-bordeaux.fr)

tel : (+33) (0) 2 23 23 63 72 fax: (+33) (0) 2 23 23 63 72

Electronic Supplementary Information (ESI) available: [details of any supplementary information available should be included here]. See DOI: 10.1039/x0xx00000x

## ABSTRACT

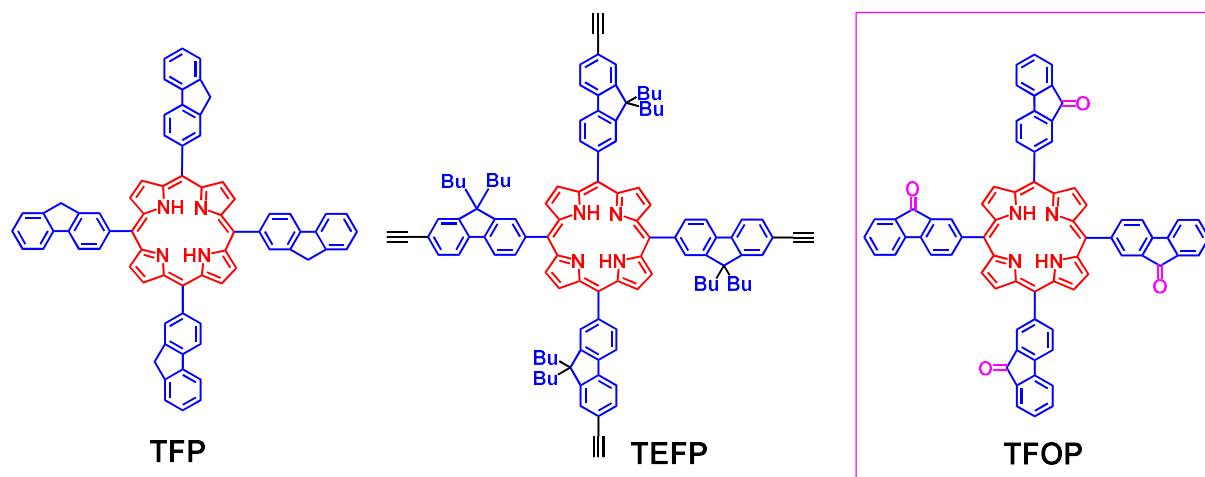
The synthesis of new *meso*-tetrafluorenylporphyrins peripherally functionalized with various 2-ethynyl fluorenyl and/or 2-ethynyl fluorenonyl arms is presented. The impact of these fluorenone units on their linear and nonlinear optical properties is also investigated. Thus, two-photon absorption and singlet oxygen photosensitising properties are evaluated. Relatively large

## Keywords

Porphyrin \* Fluorenone \* Fluorescence \* Oxygen Photosensitization \* Two-Photon Absorption

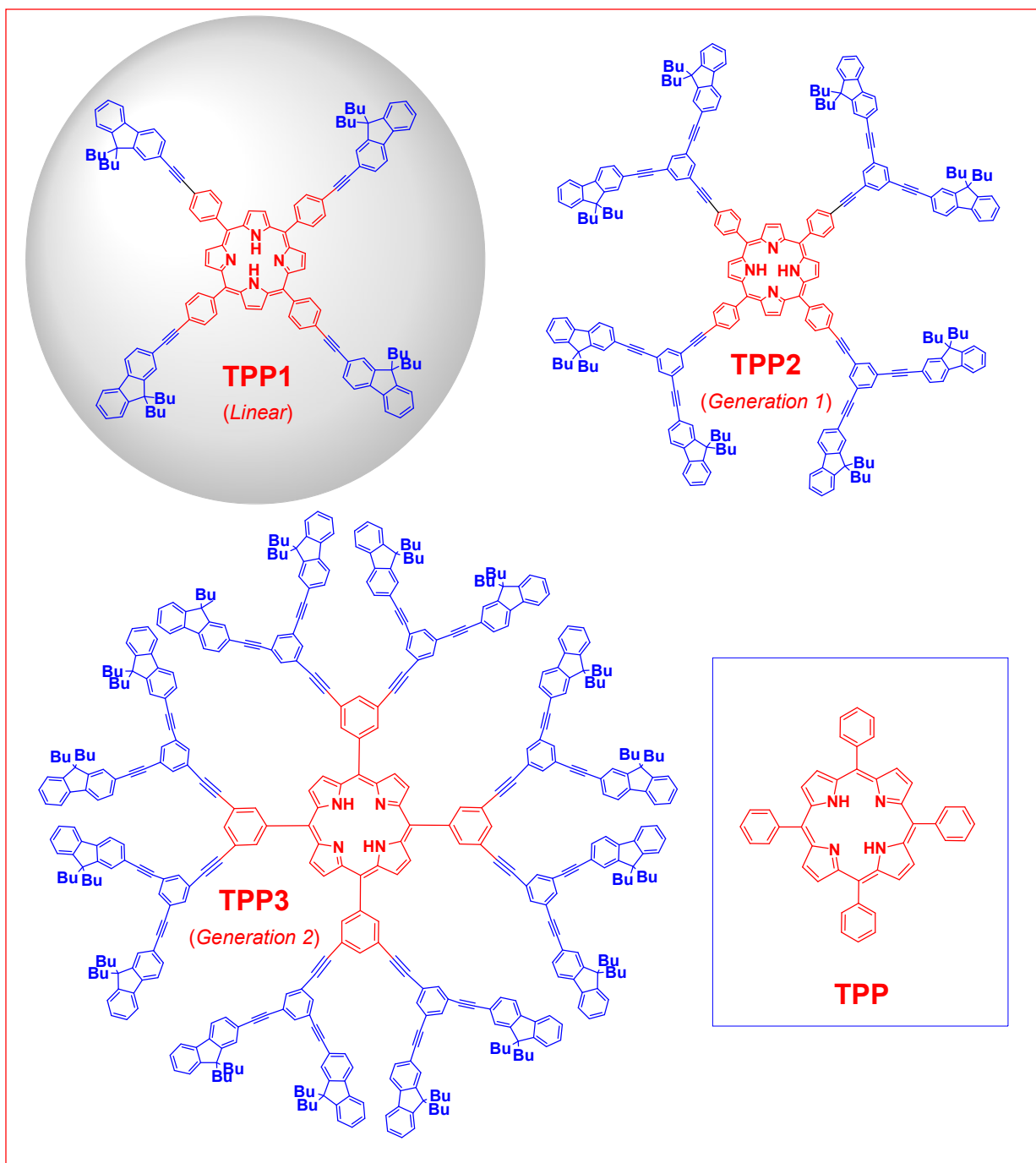
## Introduction

Porphyrins are attractive because their properties can be fine-tuned by synthetic modifications of the peripheral substituents.<sup>[1-3]</sup> In particular, we focus hereafter on a set of three new star-shaped porphyrins decorated with extra peripheral fluorenone substituents.

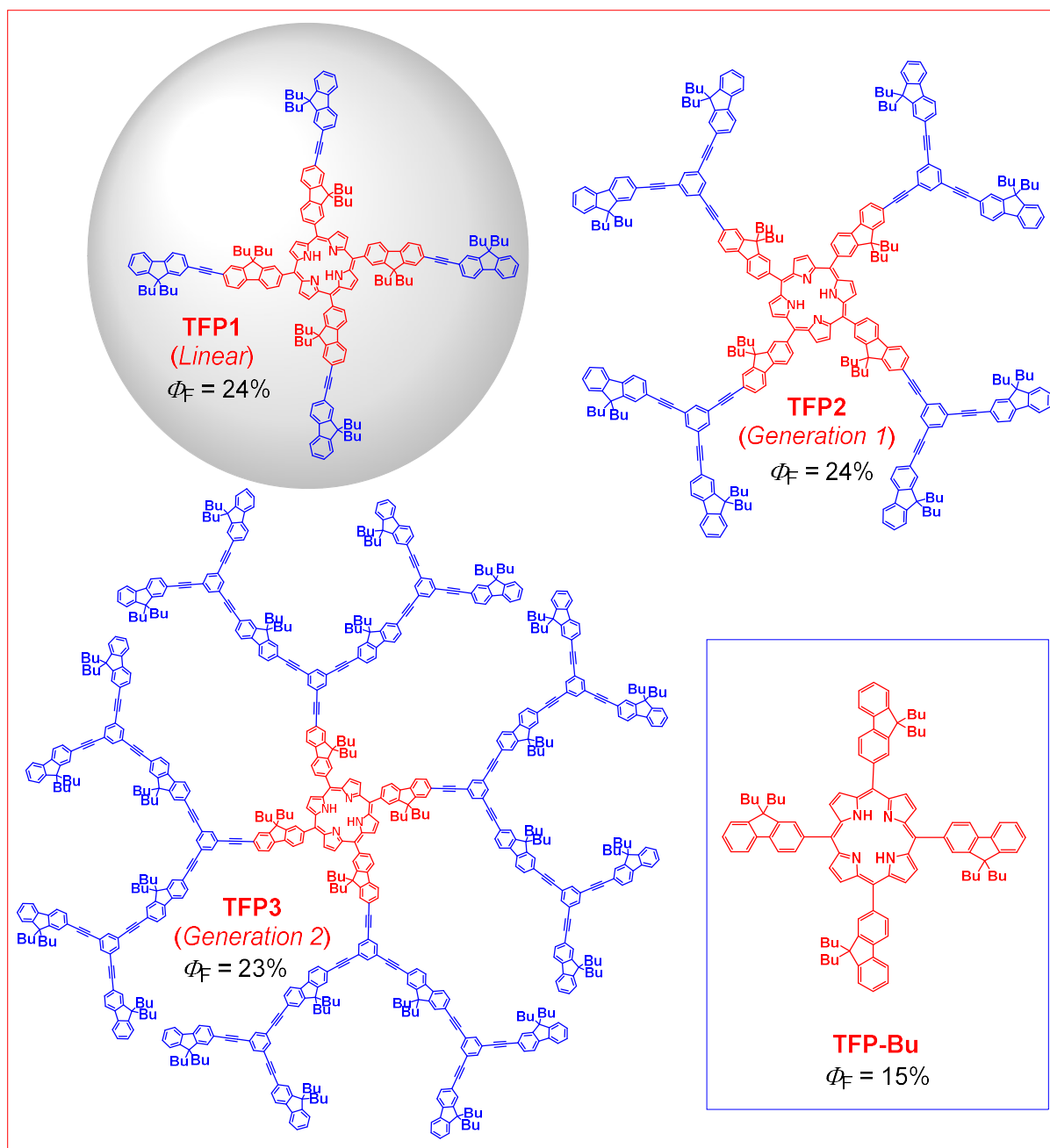


**Scheme 1.** Molecular structures of *meso*-tetrafluorenylporphyrin (**TFP**), the corresponding alkynyl-substituted compound tetra(7-ethynyl-2-fluorenyl)porphyrin (**TEFP**) and tetrafluorenylporphyrin (**TFOP**).

Accordingly, in line with independent findings of Bo and coworkers,<sup>[4]</sup> some of us had identified 5,10,15,20-tetrafluorenylporphyrin (**TFP**) as an appealing luminophore (Scheme 1).<sup>[5]</sup> As a *meso*-tetraarylporphyrin, this compound presents a remarkable quantum yield (24%) which can be ascribed to the 2-fluorenyl units. The same year we also found that a slightly higher quantum yield ( $\Phi_F = 26\%$ ) could be obtained with the 2-fluorenone analogue (**TFOP**)<sup>[6]</sup> and later on that introduction of four 2-fluorenyl units at the periphery of a *meso*-tetraphenylporphyrin core allows increasing further the light harvesting properties and luminescence quantum yield, provided that the fluorenyl units are conjugated with the central porphyrin.<sup>[7]</sup> For instance, whereas **TPP** has an emission quantum yield around 11%, **TPP1** exhibits an improved emission quantum yield of 20%. This yield can however not be further improved by attaching additional fluorenyl units at the periphery since neither **TPP2** (20%) nor **TPP3** (19%) present improved fluorescence quantum yields (Scheme 2).<sup>[7]</sup> A similar statement was also made for the dendrimer series based on a *meso*-tetrafluorenylporphyrin core (**TFP1-3** in scheme 3; see  $\Phi_F$  values).<sup>[8]</sup> In contrast, when **TFP-Bu** was functionalized with pendant ethynyl groups at its periphery, as in **TEFP** (Scheme 1), the fluorescence quantum yield dropped to 15%. This observation points to the strong influence of apparently slight structural modifications at the periphery of the **TFP** core on its emission properties.<sup>[8b]</sup>



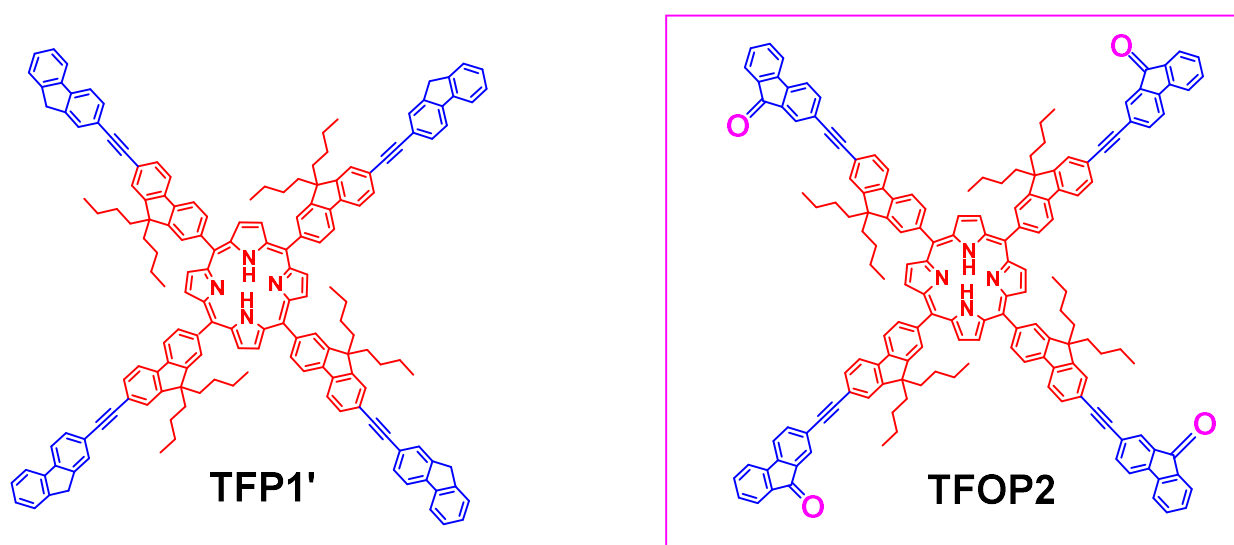
**Scheme 2.** Molecular structures of TPP-cored porphyrin dendrimers **TPP1-TPP3** and their reference **TPP**.



**Scheme 3.** Molecular structures of **TFP**-cored porphyrin dendrimers **TFP1-TFP3** and reference **TFP-Bu**.

Important two-photon absorption (2PA) cross-sections were also evidenced for all these new dendritic systems in addition to their well-known oxygen-photosensitizing capability of the tetrapyrrolic core.<sup>[9]</sup> Thus, besides applications related to OLEDs or color displays,<sup>[5b-c]</sup> we also realized that, after proper functionalization, molecular analogues of **TFP**, series **TPP1-3** or **TFP1-3** might give rise to efficient biphotonic photosensitizers for photodynamic therapy (PDT).<sup>[9,10]</sup> Due to the practical advantages of two-photon excitation, this field is rapidly

expanding and many porphyrin-based two-photon photosensitizers have been reported to date.<sup>[10,11]</sup> Such innovative developments rest on the rapid intersystem crossing taking place between the singlet and triplet excited manifolds in porphyrins (which is the first reason for their limited luminescence) and the large 2PA cross-section that related dendrimeric systems can present.<sup>[7,8,12]</sup> In our case, the intrinsic luminescence would even allow to perform simultaneous imaging, allowing an entry into so-called “two-photon theranostics”.<sup>[10b]</sup> For these applications, in addition to the optimization of their luminescence quantum yields, simultaneous optimization of their two-photon cross-section and oxygen photosensitization quantum yields are also required. In this respect, systematic structure-property studies need to be conducted on new systems. Previous such studies pointed to star-shaped structures, such as **TFP1**, for possessing the most promising potential.<sup>[8a,11a]</sup> Accordingly, we have now decided to explore the impact of the replacement of the four terminal *9H*-fluoren-2-yl (2-fluorenyl) groups by *9H*-fluoren-9-one-2-yl (2-fluorenonyl) ones on the optical properties of interest (Scheme 4).



**Scheme 4.** Molecular structures of the targeted molecule **TFOP2** vs. the reference compound **TFP1'**.

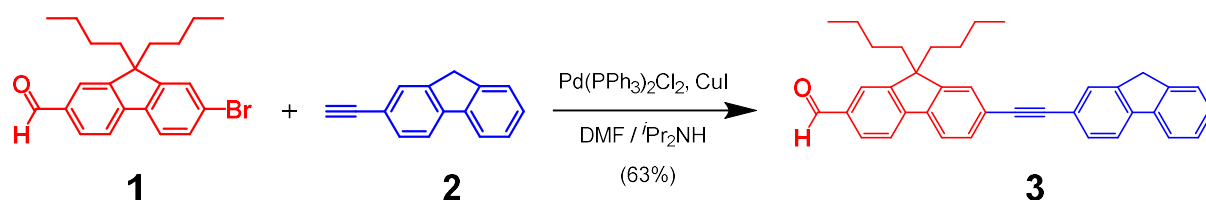
Accordingly, (i) the synthesis and characterization of two new star-shaped derivatives, **TFOP2'**, a deoxidized analogue of **TFOP2**, and **TFOP2**, and of their precursor **TFP1'** will be described first. (ii) Their electronic absorption (1PA) and emission spectra, their oxygen photosensitization properties and their 2PA spectra will next be determined. (iii) Finally, the

impact of peripheral 9-fluorenyl oxidation on the photophysical properties of **TFP1'** as well as the potential interest of **TFOP2'** and **TFOP2** for PDT will be briefly discussed.

## Results and discussion

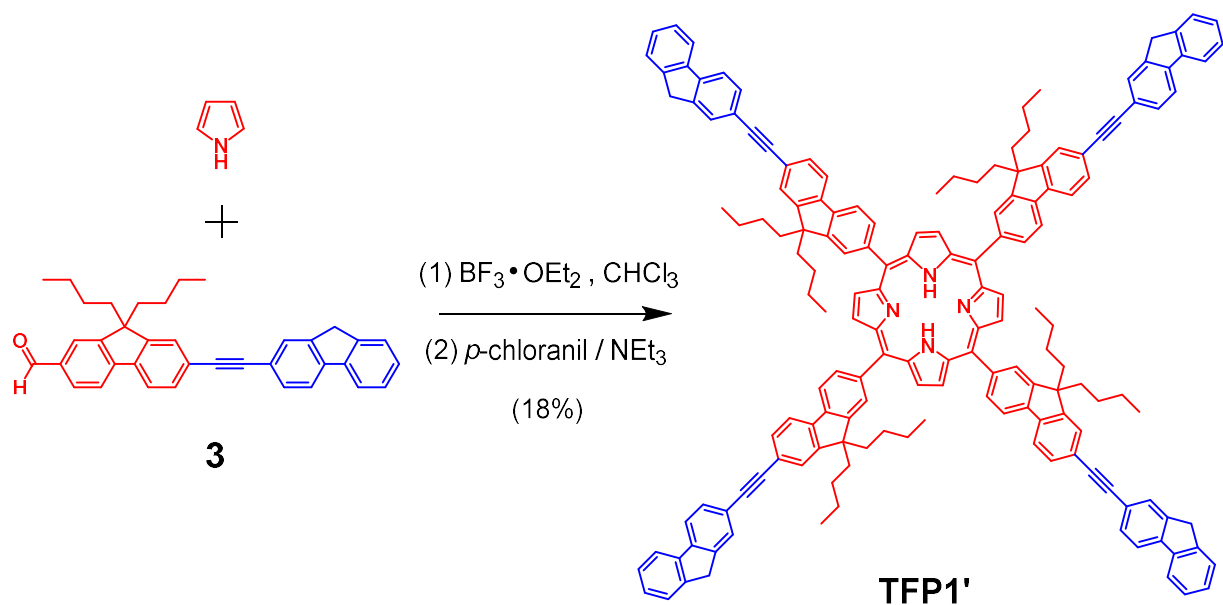
### Porphyrin synthesis

To synthesize the new star-shaped porphyrin **TFOP2** featuring four fluorenone units at its periphery, a synthetic protocol adapted from that previously used to isolate **TFOP**<sup>[6]</sup> was envisioned. Oxidation of **TFP1'** was expected to keep internal 2,7-fluorenyl units untouched and to form 2-fluorenone units specifically on external positions. During the course of this synthesis, one di-oxidized porphyrin isomer was isolated as a side-product “en route” toward **TFOP2** and also characterized. Facile synthetic access to the required precursor **TFP1'** was expected using the Lindsey method,<sup>[13]</sup> meaning that the corresponding linear difluorenyl aldehyde had to be synthesized first. This last compound (**3**) was obtained with fair yield (63%) from a Sonogashira coupling reaction<sup>[14]</sup> between the known aldehyde **1**<sup>[8a]</sup> and 2-ethynylfluorenyl **2**<sup>[7a]</sup> (Scheme 5).



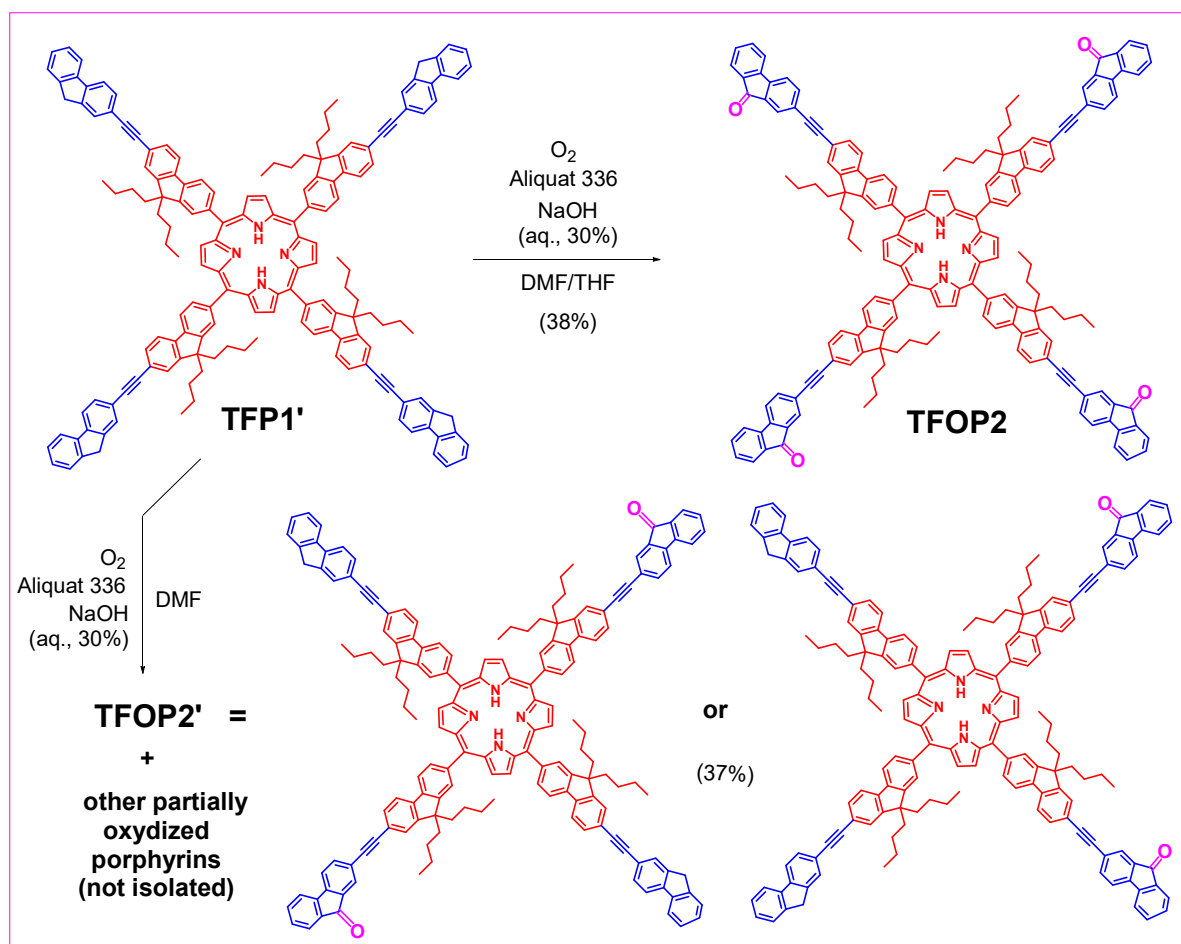
**Scheme 5.** Synthesis of the new linear difluorenyl aldehyde **3**.

From this new aldehyde **3**, the new **TFP1'** porphyrin was obtained using classic Lindsey conditions (Scheme 6).<sup>[13]</sup> and isolated in correct yield (18%), as a dark red powder after chromatographic separation.



**Scheme 6.** Synthesis of non-oxidized porphyrin **TFP1'** under Lindsey conditions.

Likewise to the synthesis of **TFOP** previously obtained by oxidation of **TFP**<sup>[6]</sup>, the desired porphyrins were obtained from **TFP1'** (Scheme 7) by aerobic oxidation in a basic biphasic (organic/aqueous) medium using Aliquat 336 as the phase transfer agent. Each time, the disappearance of the starting compound **TFP1'** was monitored by TLC to ensure completion of the reaction. The partially oxidized symmetric porphyrin **TFOP2'** was isolated in 37% as a dark red powder after chromatographic purification of the crude reaction mixture. These compounds were obtained after running the reaction in pure DMF for 59 h, while the symmetrical **A<sub>4</sub>** porphyrin **TFOP2** was obtained similarly in 38%, after running the reaction in a DMF/THF (1:1) mixture for 72 h. During the formation of **TFOP2'**, we noticed that the reaction medium contained many insolubles at the start of the reaction, whereas it is totally homogeneous in the DMF/THF solvent mixture. We believe that the formation of partially oxidized intermediates is favored when the synthesis of **TFOP2** is attempted in DMF, because this solvent does not dissolve all the precursor **TFP1'** at the start of the reaction and thus will contribute to slow down the overall oxidation reaction. As a result, only **TFOP2'** could be separated by chromatography from the reaction mixture after 59 h in DMF, while other partially oxidized intermediates that must also have been formed were not isolated.



**Scheme 7.** Synthesis of **TFOP2** and **TFOP2'** from precursor **TFP1'**.

The purity of the various porphyrin sample is established by combined mass spectrometry and elemental analysis. The new aldehyde **3** and porphyrins **TFP1'**, **TFOP2'** and **TFOP2** were characterized by  $^1H$  NMR (see ESI). Thus, for the various porphyrin derivatives, in addition to the (i)  $\beta$ -pyrrolic protons of the porphyrin core which come out as a singlet around 9 ppm and (ii) the NH protons of porphyrin cavity which come out as a second singlet around -2.5 ppm, some of the diagnostic features of the aldehyde **3** are retrieved, *i.e.* (iii) aromatic protons located as multiplets in region 8.0-7.3 ppm and (iv) alkyl protons of the various butyl chains around 2.2-0.5 ppm. In addition, for **TFP1'** and **TFOP2'**, the methylene protons of non-substituted fluorenyl groups are also observed as diagnostic singlets at 4.1 ppm. These signals progressively disappear, upon proceeding from **TFP1'** to **TFOP2**. The  $^1H$  NMR spectrum of the compound **TFOP2'** appears as a one-to-one superposition of the two previous spectra in the aromatic region. The *cis* (5,10-isomer) or *trans* (5,15-isomer) nature of the **TFOP2'** isomer isolated could not be ascertained from available data.

## Photophysical properties

In order to investigate the applied potential of these new porphyrin derivatives, we examined the absorption and emission behaviors of **TFP1'** and **TFOP2-2'** (Table 1). Their capability to photosensitize oxygen and, finally, their 2PA properties will also be subsequently measured (Table 2). During these studies, **TFP**, **TEFP** (Scheme 1), **TFP-Bu** and extended **TFP1**<sup>[8a]</sup> (Scheme 3) were chosen as reference compound to help analyzing the influence of the fluorenone groups at periphery of these star-shaped derivatives.

### Absorption spectra

The UV-visible absorption spectra of the new *para*-substituted porphyrins **TFP1'** and **TFOP2-2'** are typical for these free base porphyrins (Figure 1) with (i) an intense Soret-band around 430 nm and four Q-bands from 520-650 nm, and (ii) an extra absorption, around 310-400 nm, which corresponds to  $\pi^* \leftarrow \pi$  transitions in the conjugated arms.<sup>[7,8]</sup> This UV extra absorption, largely fluorenyl-based, is absent for **TEFP**, possibly because the less-conjugated *meso*-fluorenyl groups of **TEFP** absorb around 290 nm, whereas those of the porphyrins **TFP1'** and **TFOP2-2'**, conjugated with the porphyrin core through the ethynyl bridges, are strongly red-shifted (330-350 nm) and more intense.<sup>[8a]</sup> Related differences can also be observed between **TFP1'** (or **TFOP2-2'**) and **TFP**.<sup>[8]</sup>

**Table 1.** Photophysical properties data of the new series of fluorenone porphyrins: reference **TEFP**, non-oxidized **TFP1'** and **TFOP2-2'** in CH<sub>2</sub>Cl<sub>2</sub> (HPLC quality) at R.T.

	$\lambda_{\text{dendron}}$ /nm	$\lambda_{\text{Soret}}$ / nm	$\lambda_{\text{Q-bands}}$ / nm	$\lambda_{\text{em}}$ / nm	$\Phi_{\text{F}}$ <sup>a</sup> / %	$\tau$ / ns
<b>TEFP</b>	292	428	520, 558, 594, 652	660, 724	15	8.2
<b>TFP1'</b>	340	431	521, 559, 596, 652	660, 725	<b>22</b>	8.0
<b>TFOP2'</b>	315, 346	431	521, 558, 596, 652	660, 725	<b>21</b>	8.0
<b>TFOP2</b>	310, 352	431	521, 560, 596, 652	660, 724	<b>22</b>	8.0

<sup>a</sup> Fluorescence quantum yield determined relative to **TPP** in toluene.

After normalizing the spectra on the Soret-band intensity, the dendron-based absorption clearly separates in two parts when going from **TFP1'** to **TFOP2**, *i.e.* with increasing fluorenone units (Figure 1), while the porphyrin-based transitions (Soret-band and Q-bands) remain constant. It can also be noticed that the intensity of the first dendron-based absorption gets weaker and larger with the increasing number of fluorenone units, suggesting that fluorenone sub-chromophores in **TFOP2** and **TFOP2'** behave as weaker absorbers than do terminal fluorene units.

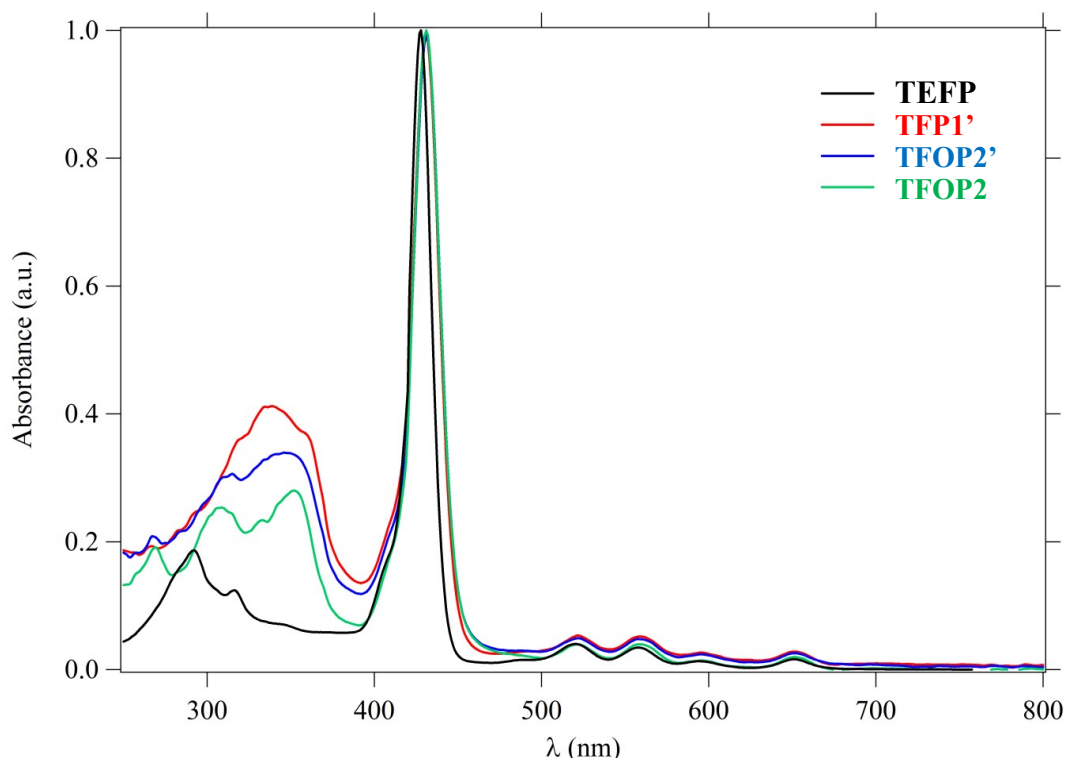


**Figure 1.** UV-visible spectra of porphyrins **TFP1'**, **TFOP2-2'** and reference **TFP** in  $\text{CH}_2\text{Cl}_2$ .

### Emission spectra

Upon excitation in their Soret-band, **TFP1'**, **TFOP2-2'** and the reference compound **TFP** exhibit the characteristic porphyrin emission peaks Q(0,0) and Q(0,1).<sup>[7,8]</sup> After normalizing the emission intensities of the various compounds on their Q(0,0) peaks, all four compounds exhibit similar emission spectra (Figure 2a). Then, for **TFP1'** and **TFOP2-2'**, the intensity ratios between Q(0,0) and Q(0,1) remain constant, as previously observed for the porphyrin-cored dendrimers.<sup>[7,8]</sup> All three compounds **TFP1'** and **TFOP2-2'** show slightly lower quantum yields ( $\Phi_F \sim 22\%$ ) than TFP-cored porphyrin dendrimers **TFP1-3** ( $\sim 24\%$ ).<sup>[8a]</sup> However, when compared to the TPP-cored porphyrins **TPP1-3** ( $\sim 20\%$ ),<sup>[7]</sup> their luminescence

quantum yields are slightly higher of *ca.* 2%, in contrast to the *tetra*-alkynyl porphyrin **TEFP** (Table1).

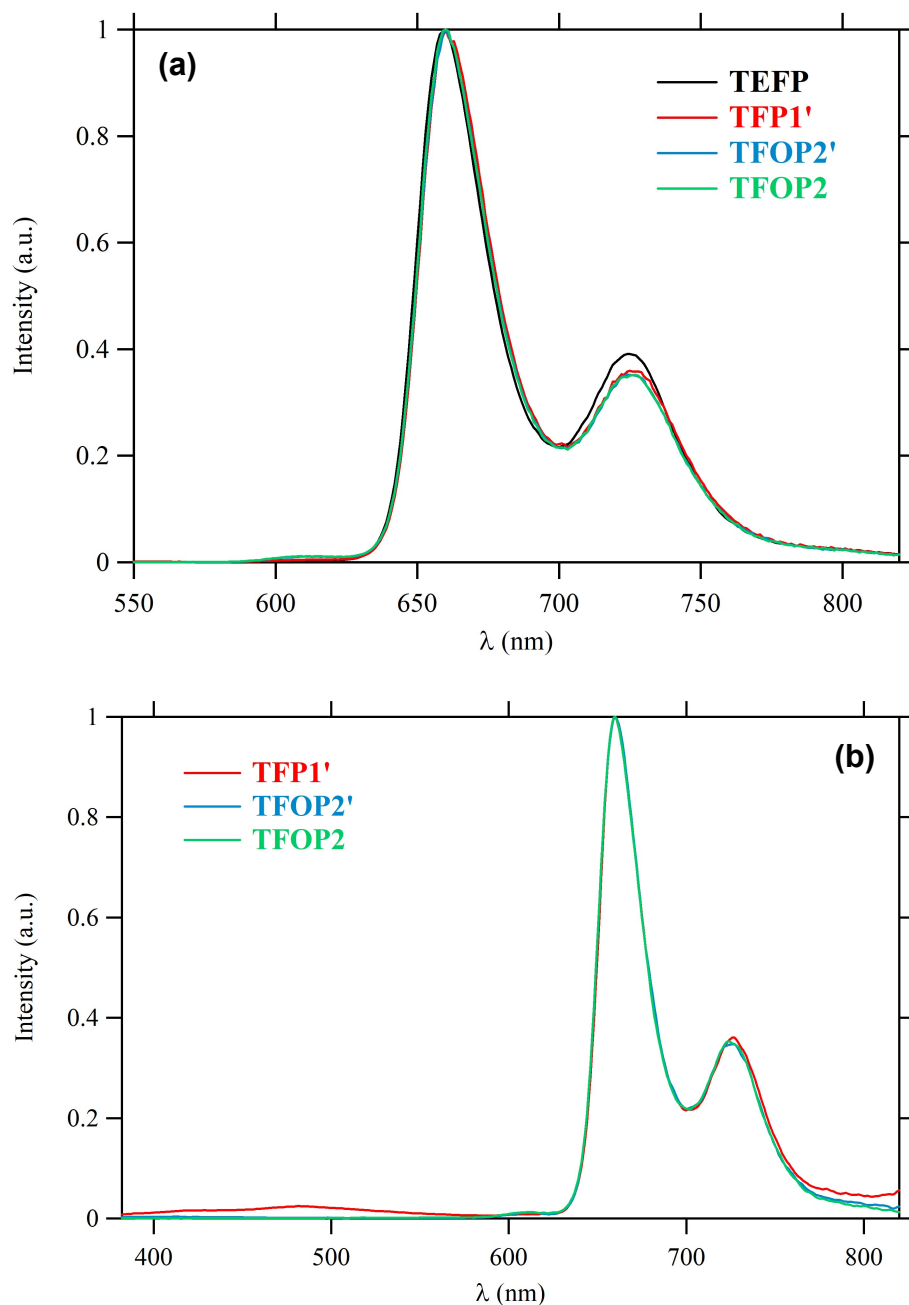


**Figure 2.** a) Normalized emission spectra of **TEFP**, **TFP1'** and **TFOP2-2'** in  $\text{CH}_2\text{Cl}_2$  (500-820 nm) after excitation in their Soret band; b) Complete normalized emission spectra of **TFP1'** and **TFOP2-2'** excited in their arm-based absorption (380 nm). Corresponding non-normalized spectra are provided in the ESI.

## Energy Transfer from conjugated arms to porphyrin core

The existence of an energy transfer (ET) between the peripheral arms and the central porphyrin core was also probed. Figure 2b presents the emission spectra of **TFP1'** and **TFOP2-2'** upon UV excitation in the arm-based absorption (~380 nm). The resulting emission spectra show only the red emission (at 660 and 725 nm), characteristic of the porphyrin core, and no residual blue emission, characteristic of the arm, meaning that the dendron emission is completely quenched through an efficient process most likely corresponding to a through-bond ET (TBET)<sup>[15]</sup> from the peripheral fluorenone moieties to the porphyrin core via the fluorene perpendicular connectors.

## Oxygen Sensitization

We next wondered about the oxygen-sensitizing capabilities of **TFP1'** and **TFOP2-2'**. The quantum yields of singlet oxygen generation were therefore determined for these compounds and compared to those of **TFP1**<sup>[8a]</sup> (Table 2). All the new compounds exhibit values ( $\Phi_{\Delta} \sim 65\%$ ) higher than that of **TFP1** ( $\Phi_{\Delta} = 62\%$ ). Interestingly, these measurements reveal that the high fluorescence efficiency of the porphyrins (especially in comparison with model **TPP**) is not obtained at the expense of the singlet oxygen production.

**Table 2.** Photophysical properties of **TFP**-cored porphyrins and relevant reference compounds.

Compound	$\lambda_{\text{abs}}$ (Soret) (nm)	$\epsilon$ ( $\text{M}^{-1}\text{cm}^{-1}$ )	$\lambda_{\text{em}}$ (nm)	$\Phi_{\text{F}}$ <sup>a</sup>	$\Phi_{\text{F}}$ <sup>b</sup>	$\Phi_{\Delta}$ <sup>c</sup>	$\sigma_2$ <sup>d</sup> (GM)
<b>TFP</b>	425	–	659, 724	0.24	0.24	0.60	90
<b>TFP-Bu</b>	426	–	660, 724	0.18	0.20	0.64	140
<b>TFP1</b>	432	669 000	660, 726	0.23	0.24	0.62	770
<b>TFP1'</b>	431	477 000	660, 726	0.21	0.22	0.66	530
<b>TFOP2'</b>	<b>431</b>	<b>578 000</b>	<b>660, 726</b>	<b>0.21</b>	<b>0.21</b>	<b>0.65</b>	<b>640</b>
<b>TFOP2</b>	<b>431</b>	<b>509 000</b>	<b>660, 726</b>	<b>0.21</b>	<b>0.22</b>	<b>0.64</b>	<b>610</b>

<sup>a</sup>Fluorescence quantum yield in dichloromethane determined relative to **TPP** in toluene. <sup>b</sup>Fluorescence quantum yield in toluene. <sup>c</sup>Singlet oxygen formation quantum yield determined relative to tetraphenylporphyrin in dichloromethane ( $\Phi_{\Delta}[\text{TPP}] = 0.60$ ). <sup>d</sup>Intrinsic 2PA cross-sections at 790 nm in dichloromethane, measured by TPEF in the femtosecond regime; a fully quadratic dependence of the fluorescence intensity on the excitation power is observed and 2PA responses are fully non-resonant ( $\lambda_{\text{exc}} \geq 790$  nm).

## Two-Photon Absorption

Given the important 2PA cross-sections previously evidenced **TFP1** and **TFP1** (Schemes 2 and 3),<sup>[7,8a]</sup> we finally turned our attention to the 2PA properties of **TFP1'** and **TFOP2-2'** (which exhibit quite similar two-photon absorptivities). Taking advantage of their good fluorescence, the 2PA cross-sections of these TFP-cored compounds were determined by two-photon excited fluorescence (TPEF). Measurements were performed with  $10^{-4}$  M solutions, using a mode-locked Ti:sapphire laser delivering femtosecond pulses, following the experimental protocol described by Xu and Webb.<sup>[16]</sup> A fully quadratic dependence of the fluorescence intensity on the excitation power was observed for each sample at all the wavelengths of the spectra shown in Figure 3, indicating that the cross-sections determined are only due to 2PA. A significant increase of the 2PA cross-sections compared to that of **TFP** (12 GM at 790 nm) was observed for all the new porphyrins (Table 2).

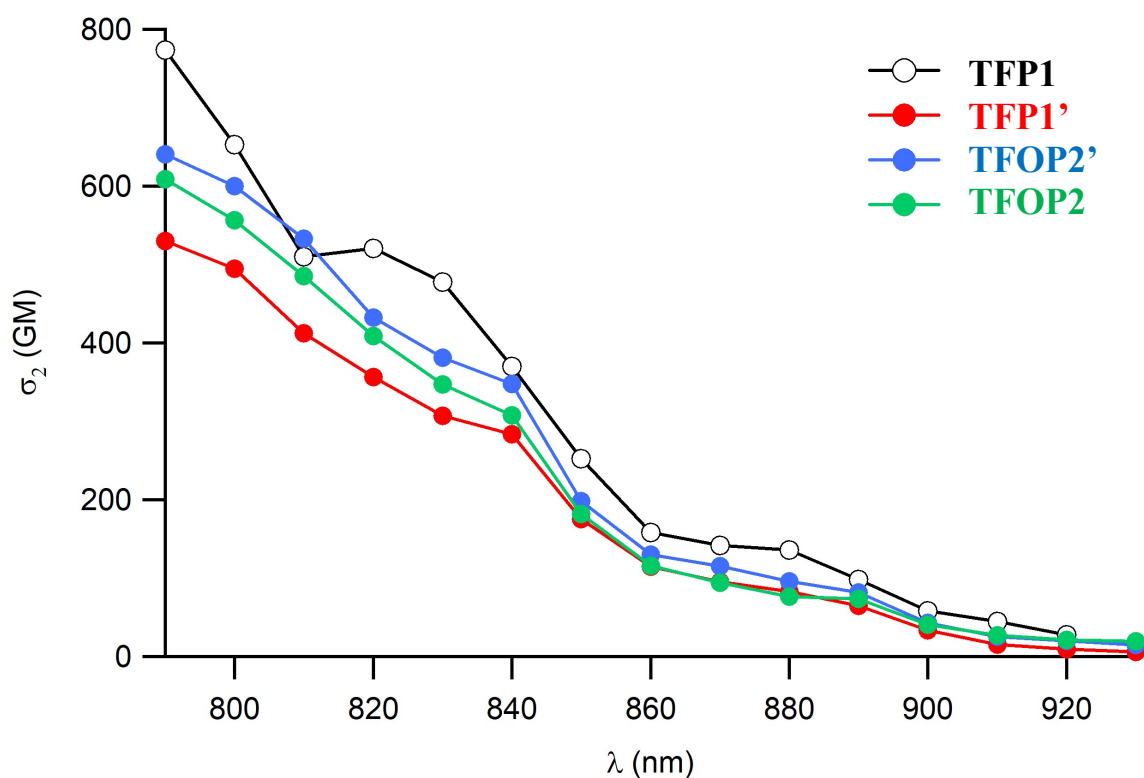


**Figure 3.** Two-Photon Absorption Spectra for TFP-cored compounds **TFP1'** and **TFOP2-2'** compared to **TFP1** in  $\text{CH}_2\text{Cl}_2$ .

We have shown earlier that replacing the four phenyl groups at *meso*-positions by four fluorenyl groups leads to a clear improvement in the 2PA properties.<sup>[7,8]</sup> When comparing

TFP-cored porphyrins together, it appears that butyl chains on the *meso*-fluorenyl groups of the porphyrin in **TFP-Bu** (140 GM) favor TPA over bare fluorenyl arms in **TFP** (90 GM). Similarly, 2-fluorenone units appears more efficient for promoting 2PA than bare 2-ethynylfluorenyl groups at 7-positions of *meso*-fluorenyl groups in **TFP1'** (530 GM). Thus, a **TFP-Bu** core decorated with such units (**TFP1'**) is a worst two-photon absorber than **TFOP2-2'** (610-640 GM) or **TFP1** (770 GM).

## Conclusions

The synthesis and characterization of two conjugated *meso*-tetrafluorenylporphyrin-cored compounds peripherally functionalized with additional ethynyl-2-fluorenyl/fluorenon-2-yl units (**TFOP2-2'**) has been reported here. These new star-shaped derivatives were easily obtained by aerobic oxidation of the non-oxidized porphyrin precursor **TFP1'**. In terms of photophysical properties, all three new porphyrins exhibit remarkably high luminescence quantum yields ( $\Phi_F \sim 21\text{-}22\%$ ) for *meso*-tetraarylporphyrins and present also a potentially large brightness, thanks to the very efficient energy transfer from the peripheral arms units toward the central porphyrin core (TBET). While these high luminescence quantum yields make them potentially interesting for organic light emitting devices, these compounds behave also as efficient photosensitizers for oxygen, with quantum yields of singlet oxygen generation around 65% *i.e.* higher to that previously reported for **TFP1** ( $\Phi_\Delta = 62\%$ ). Interestingly, their high fluorescence quantum yields (especially in comparison with the **TFP** model compound) are not obtained at the expense of the singlet oxygen production. Finally, their 2PA cross-sections of **TFP1'** and **TFOP2-2'**, when compared to that of **TFP** (90 GM), are much larger ( $\sim 600$  GM) pointing to the beneficial impact of increasing the size of the  $\pi$ -manifold in the peripheral arms. Actually, **TFOP2** and **TFOP2'** exhibit quite similar two-photon absorptivities (640-610 GM), which are significantly higher than for the non-oxidized compound **TFP1'** (530 GM), in line with a beneficial role of 2-fluorene for 2-fluorenone replacement on nonlinear absorption properties. Thus, combined to their remarkable fluorescence quantum yields and oxygen-photosensitizing properties, their rather large 2PA cross-sections make them potentially interesting for applications in theranostics. After proper functionalization, this type of structure should, likewise to related systems recently developed for such uses,<sup>[10b,11]</sup> give rise to original porphyrin-based molecular assemblies combining two-photon PDT and two-photon fluorescence imaging. In connection with previous results,<sup>[11b]</sup> the replacement of peripheral

9,9-dibutyl-9*H*-fluoren-2-yl units by units by 9*H*-fluoren-9-one-2-yl units in the corresponding water-soluble star-shaped analogues should therefore not drastically affect their 2PA cross-section, nor their relevant linear optical properties. However, other important properties such as their solubility, self-aggregation or bio-distribution might be more profoundly modified. As such, oxidation of the peripheral 2-fluorenyl units should be envisioned as a potential mean to improve the overall efficiency of two-photon photosensitizers related to **TFP1'** or **TFP1**.

## Experimental Section

### General

Unless otherwise stated, all solvents used in reactions were distilled using common purification protocols,<sup>[17]</sup> except DMF and <sup>i</sup>Pr<sub>2</sub>NH which were dried on molecular sieves (3 Å). Compounds were purified by chromatography on silica gel using different mixtures of eluents as specified. <sup>1</sup>H and <sup>13</sup>C NMR spectra were recorded on BRUKER Ascend 400 and 500 at 298 K. The chemical shifts are referenced to internal tetramethylsilane. High-resolution mass spectra were recorded on different spectrometers: a Bruker MicrOTOF-Q II, a Thermo Fisher Scientific Q-Exactive in ESI positive mode and a Bruker Ultraflex III MALDI Spectrometer at CRMPO (centre regional de mesures physiques de l'Ouest) in Rennes. Reagents were purchased from commercial suppliers and used as received. Compounds 7-bromo-9,9-dibutyl-fluorene-2-carboxaldehyde (**1**)<sup>[8a]</sup> and 2-ethynyl-fluorene (**2**),<sup>[7b]</sup> were synthesized as described earlier, using an adapted approach for **2** (ESI).

### Synthesis of organic precursors

**Difluorenyl aldehyde 3.** In a Schlenk tube, a mixture of 7-bromo-9,9-dibutyl-fluorene-2-carboxaldehyde (**1**) (492 mg, 1.28 mmol, 1 equiv), 2-ethynyl-fluorene (**2**) (365 mg, 1.92 mmol, 1.5 equiv), Pd(PPh<sub>3</sub>)<sub>2</sub>Cl<sub>2</sub> (5.4 mg, 0.008 mmol, 0.6% equiv.) and CuI (excess) were dissolved in DMF (5 mL) and then <sup>i</sup>Pr<sub>2</sub>NH (5 mL) was added under argon. The reaction

medium was degassed by freeze-pump-thaw twice and heated for 48h at 95 °C. After evaporation of the volatiles, residue was further purified by silica chromatography using heptane as eluent; the desired aldehyde **3** (398 mg, 63% yield) was obtained as a yellow powder. <sup>1</sup>H NMR (400 MHz, CDCl<sub>3</sub>): δ = 10.07 (s, 1H, H<sub>CHO</sub>), 7.89-7.76 (m, 7H, H<sub>fluorenyl</sub>), 7.63-7.57 (m, 3H, H<sub>fluorenyl</sub>), 7.43-7.31 (m, 3H, H<sub>fluorenyl</sub>), 3.94 (s, 2H, H<sub>9-fluorenyl</sub>), 2.10-1.99 (m, 4H, H<sub>a</sub>), 1.16-1.04 (m, 4H, H<sub>c</sub>), 0.70-0.44 (m, 10H, H<sub>b</sub>, H<sub>d</sub>). <sup>13</sup>C NMR (100 MHz, CDCl<sub>3</sub>, ppm): δ = 186.5, 161.0, 157.6, 156.2, 155.2, 150.9, 150.6, 149.0, 143.1, 139.5, 139.1, 138.3, 137.8, 133.6, 131.2, 130.7, 128.3, 105.1, 99.5, 99.4, 41.5, 40.4, 33.2, 23.9, 11.1. HRMS-ESI for C<sub>37</sub>H<sub>35</sub>O: m/z = 495.2680 [M+H]<sup>+</sup> (calcd: 495.26824).

**Porphyrin TFPI'**. In a two-neck flask, a mixture of previously prepared difluorenyl aldehyde **3** (564 mg, 1.14 mmol, 1 equiv.) and pyrrole (0.08 mL, 1.14 mmol, 1 equiv.) were dissolved in distilled chloroform (250 mL) under argon. After degassing the mixture with argon bubbling for 30 min, BF<sub>3</sub>•OEt<sub>2</sub> (0.04 mL, 0.29 mmol, 0.25 equiv.) was injected and the reaction was stirred in dark for 3 h under argon at room temperature. Then oxidant *p*-chloranil (210 mg, 0.86 mmol, 0.75 equiv.) was added, and the reaction was heated at 45 °C for another 1 h without any protection. After cooling the reaction to room temperature, NEt<sub>3</sub> (2 mL) was injected, and then keep stirring for several minutes. After evaporation of the volatiles, purification was done by silica gel chromatography using THF/heptane (1:4) mixture as eluents, the porphyrin **TFPI'** was collected as violet powder (110 mg, 18% yield). MP: 216-218°C (dec). Rf: 0.72 (THF/Heptane [1:1]). <sup>1</sup>H NMR (300 MHz, THF-*d*<sub>8</sub>): δ = 8.94 (s, 8H, H<sub>β-pyrrolic</sub>), 8.31-8.24 (m, 8H, H<sub>1,3</sub>), 8.18 (d, 4H, *J* = 7.8 Hz, H<sub>4</sub>), 8.04 (d, 4H, *J* = 8.1 Hz, H<sub>5</sub>), 7.87-7.83 (m, 8H, H<sub>10,12</sub>), 7.76 (d, 4H, *J* = 8.4 Hz, H<sub>6,8</sub>), 7.67 (d, 4H, *J* = 7.8 Hz, H<sub>13</sub>), 7.61-7.55 (m, 8H, H<sub>14,17</sub>), 7.39-7.27 (m, 8H, H<sub>15,16</sub>), 3.95 (s, 8H, H<sub>18</sub>), 2.25 (s, 16H, H<sub>a</sub>), 1.28-1.19 (m, 16H, H<sub>c</sub>), 1.10-0.94 (m, 16H, H<sub>b</sub>), 0.83-0.77 (m, 24H, H<sub>d</sub>), -2.50 (s, 2H, NH). <sup>13</sup>C NMR (100 MHz, CDCl<sub>3</sub>, ppm): δ = 151.2, 149.4, 143.7, 143.4, 141.9, 141.5, 141.3, 141.0, 140.4, 133.5, 130.7, 130.2, 129.3, 128.6, 127.9, 127.0, 126.7, 125.9, 124.8, 122.5, 121.6, 120.6, 120.1, 119.9, 119.7, 118.2, 90.4, 90.2, 55.2, 40.1, 36.2, 29.6, 26.4, 13.4. HRMS-ESI for C<sub>164</sub>H<sub>143</sub>N<sub>4</sub> : m/z = 2168.1231 [M+H]<sup>+</sup> (calcd: 2168.13073). Anal. Calcd. (%) for C<sub>164</sub>H<sub>142</sub>N<sub>4</sub>·3THF: C 88.62; H 7.01; N 2.35. Found: C 88.71; H 7.15; N, 2.32.

**Partially Oxidized porphyrin TFOP2'.** In a two-neck flask, non-oxidized **TFP1'** (50 mg, 0.02 mmol, 1 equiv.) is dissolved in 1 mL of DMF. Aqueous NaOH (30%, 4.6 mL) is carefully added, followed by addition of Aliquat 336 (tricaprylmethylammonium chloride). The mixture is stirred for 59 h. Reaction progress is monitored by TLC, spotting directly from the organic layer. Then, the dark violet solution is separated and concentrated. The crude is chromatographed on silica gel column with THF/heptane (1:4) as eluent, the title porphyrin is obtained as dark violet powder (19 mg, 37% yield). MP: 238-240 °C (dec). Rf: 0.56 (THF/Heptane [1:1]). <sup>1</sup>H NMR (300 MHz, THF-*d*<sub>8</sub>): δ = 8.93 (s, 8H, H<sub>β-pyrrolic</sub>), 8.34-8.18 (m, 12H, H<sub>1,3,4</sub>, H<sub>1',3',4'</sub>), 8.07-8.03 (m, 4H, H<sub>5</sub>, H<sub>5'</sub>), 7.87-7.82 (m, 6H, H<sub>fluorenyl</sub>, fluorenone), 7.76 (d, 8H, *J* = 8.7 Hz, H<sub>6,8</sub>, H<sub>6',8'</sub>), 7.72-7.64 (m, 8H, H<sub>fluorenyl</sub>, fluorenone), 7.61-7.54 (m, 8H, H<sub>fluorenyl</sub>, fluorenone), 7.39-7.27 (m, 8H, H<sub>15,16</sub>, H<sub>15',16'</sub>), 3.96 (s, 8H, H<sub>18</sub>), 2.25 (s, 16H, H<sub>a</sub>, H<sub>a'</sub>), 1.25-1.16 (m, 16H, H<sub>c</sub>, H<sub>c'</sub>), 1.10-0.93 (m, 16H, H<sub>b</sub>, H<sub>b'</sub>), 0.87-0.77 (m, 24H, H<sub>d</sub>, H<sub>d'</sub>), -2.50 (s, 2H, NH). UV-vis (λ<sub>max</sub>, CH<sub>2</sub>Cl<sub>2</sub>, nm): 351, 431, 521, 560, 596, 652. HRMS-ESI for C<sub>164</sub>H<sub>139</sub>N<sub>4</sub>O<sub>2</sub>: *m/z* = 2196.0847 [M+H]<sup>+</sup> (calcd: 2196.08926). Anal. Calcd. (%) for C<sub>164</sub>H<sub>138</sub>N<sub>4</sub>O<sub>2</sub>·3THF: C 87.60; H 6.77; N 2.32. Found: C 87.98; H 6.52; N, 2.25.

**Fully-Oxidized Porphyrin TFOP2.** In a two-neck flask, non-oxidized **TFP1'** (36 mg, 0.02 mmol, 1 equiv.) is dissolved in DMF (1 mL) and THF (1 mL). Aqueous NaOH (30%, 4.6 ml) is carefully added, followed by addition of Aliquat 336 (tricaprylmethylammonium chloride). The mixture is stirred for 72 h. Reaction progress is monitored by TLC, spotting directly from the organic layer. Then, the dark violet solution is separated and concentrated. The crude is chromatographed on silica gel column with THF/heptane (1:1) as eluent, **TFOP2** is obtained as dark violet powder (14 mg, 38% yield). MP: 237-239 °C (dec). Rf: 0.40 (THF/Heptane [1:1]). <sup>1</sup>H NMR (300 MHz, THF-*d*<sub>8</sub>): δ = 8.93 (s, 8H, H<sub>β-pyrrolic</sub>), 8.32-8.25 (m, 8H, H<sub>1,3</sub>), 8.19 (d, 4H, *J* = 7.8 Hz, H<sub>4</sub>), 8.05 (d, 4H, *J* = 7.8 Hz, H<sub>5</sub>), 7.82-7.64 (m, 28H, H<sub>fluorenyl</sub>, fluorenonyl), 7.77-7.74 (m, 12H, H<sub>6,8,12</sub>), 7.71-7.64 (m, 8H, H<sub>13,14,17</sub>), 7.56 (t, 4H, *J* = 8.0 Hz, H<sub>15</sub>), 7.36 (t, 4H, *J* = 7.4 Hz, H<sub>16</sub>), 2.25 (t, *J* = 7.8 Hz, 16H, H<sub>a</sub>), 1.26-1.16 (m, 16H, H<sub>c</sub>), 1.11-0.93 (m, 16H, H<sub>b</sub>), 0.82-0.77 (m, 24H, H<sub>d</sub>), -2.50 (s, 2H, NH). <sup>13</sup>C NMR (100 MHz, CDCl<sub>3</sub>, ppm): δ = 193.5, 153.2, 151.4, 145.8, 145.6, 143.6, 143.5, 142.1, 139.1, 136.6, 136.2, 135.3, 132.8, 131.2, 128.2, 128.0, 126.2, 125.7, 123.6, 122.6, 122.5, 122.4, 122.0, 120.2, 93.8, 90.6, 57.2, 31.5, 28.3, 24.9, 15.3. HRMS-ESI for C<sub>164</sub>H<sub>135</sub>N<sub>4</sub>O<sub>4</sub>: *m/z* = 2224.0442 [M+H]<sup>+</sup>

(calcd: 2224.04778). Anal. Calcd. (%) for C<sub>164</sub>H<sub>134</sub>N<sub>4</sub>O<sub>4</sub>·3THF: C 86.59; H 6.52; N 2.30. Found: C 86.56; H 6.57; N, 2.07.

## Spectroscopic Measurements

All photophysical measurements have been performed with freshly-prepared air-equilibrated solutions at room temperature (298 K). UV-Vis absorption spectra were recorded on a Jasco V-570 spectrophotometer. Steady-state fluorescence measurements were performed on dilute solutions (ca. 10<sup>-6</sup> M, optical density < 0.1) contained in standard 1 cm quartz cuvettes using an Edinburgh Instrument (FLS920) spectrometer in photon-counting mode. Fully corrected emission spectra were obtained, for each compound, after excitation at the wavelength of the absorption maximum, with  $A_{\lambda_{\text{ex}}} < 0.1$  to minimize internal absorption.

## Measurements of singlet oxygen quantum yield ( $\Phi_{\Delta}$ )

Measurements were performed on a Fluorolog-3 (Horiba Jobin Yvon), using a 450 W Xenon lamp. The emission at 1272 nm was detected using a liquid nitrogen-cooled Ge-detector model (EO-817L, North Coast Scientific Co). Singlet oxygen quantum yields  $\Phi_{\Delta}$  were determined in dichloromethane solutions, using tetraphenylporphyrin (TPP) in dichloromethane as reference solution ( $\Phi_{\Delta}[\text{TPP}] = 0.60$ ) and were estimated from <sup>1</sup>O<sub>2</sub> luminescence at 1272 nm.

## Two-Photon Absorption Experiments

To span the 790-920 nm range, a Nd:YLF-pumped Ti:sapphire oscillator (Chameleon Ultra, Coherent) was used generating 140 fs pulses at a 80 MHz rate. The excitation power is controlled using neutral density filters of varying optical density mounted in a computer-controlled filter wheel. After five-fold expansion through two achromatic doublets, the laser beam is focused by a microscope objective (10×, NA 0.25, Olympus, Japan) into a standard 1 cm absorption cuvette containing the sample. The applied average laser power arriving at the sample is typically between 0.5 and 40 mW, leading to a time-averaged light flux in the focal volume on the order of 0.1–10 mW/mm<sup>2</sup>. The fluorescence from the sample is collected in epifluorescence mode, through the microscope objective, and reflected by a dichroic mirror

(Chroma Technology Corporation, USA; “blue” filter set: 675dxcru; “red” filter set: 780dxcr). This makes it possible to avoid the inner filter effects related to the high dye concentrations used ( $10^{-4}$  M) by focusing the laser near the cuvette window. Residual excitation light is removed using a barrier filter (Chroma Technology; “blue”: e650–2p, “red”: e750sp–2p). The fluorescence is coupled into a 600  $\mu\text{m}$  multimode fiber by an achromatic doublet. The fiber is connected to a compact CCD-based spectrometer (BTC112-E, B&W Tek, USA), which measures the two-photon excited emission spectrum. The emission spectra are corrected for the wavelength-dependence of the detection efficiency using correction factors established through the measurement of reference compounds having known fluorescence emission spectra. Briefly, the set-up allows for the recording of corrected fluorescence emission spectra under multiphoton excitation at variable excitation power and wavelength. TPA cross sections ( $\sigma_2$ ) were determined from the two-photon excited fluorescence (TPEF) cross sections ( $\sigma_2 \cdot \Phi_F$ ) and the fluorescence emission quantum yield ( $\Phi_F$ ). TPEF cross sections of  $10^{-4}$  M dichloromethane solutions were measured relative to fluorescein in 0.01 M aqueous NaOH using the well-established method described by Xu and Webb<sup>[16]</sup> and the appropriate solvent-related refractive index corrections.<sup>[18]</sup> The quadratic dependence of the fluorescence intensity on the excitation power was checked for each sample and all wavelengths.

**Supporting Informations.** Synthetic details,  $^1\text{H}$  NMR and mass spectra of all new compounds. This material is available free of charge via the Internet at <http://pubs.acs.org>.

## Conflict of Interest

## Acknowledgements

The authors acknowledge CNRS for their financial support and China Scholarship Council (CSC) for PhD funding (XZ and ZS). This project was supported by the departmental committees CD35, CD28 and CD29 of the “*Ligue contre le Cancer du Grand-Ouest*”. We also thank Guillaume Clermont (ISM) for his help in the two-photon and singlet oxygen measurements.

## References

- 1 W.-Y. Wong and C.-L. Ho, *Coord. Chem. Rev.*, **2009**, 253, 1709-1753.
- 2 Zang, X. H.; Xie, Z. Y.; Wu, F. P.; Zhou, L. L.; Wong, O. Y.; Lee, C. S.; Kwong, H. L.; Lee, S. T.; Wu, S. K. *Chem. Phys. Lett.* **2003**, 382, 561-566.
- 3 a) Baldo, M. A.; O'Brien, D. F.; You, Y.; Shoustikov, A.; Sibley, S.; Thompson, M. E.; Forrest, S. R. *Nature* **1998**, 395, 151-154; b) Virgili, T.; Lidzey, D. G.; Bradley, D. D. C. *Synth. Metals* **2000**, 111-112, 203-206.
- 4 a) Z. Fei, B. Li, Z. Bo, R. Lu, *Org. Lett.* **2004**, 6, 4703 - 4706; b) B. Li, J. Li, Y. Fu, Z. Bo, *J. Am. Chem. Soc.*, **2004**, 126, 3430-3436; c) B. Li, X. Xu, M. Sun, Y. Fu, G. Yu, Y. Liu, Z. Bo, *Macromolecules*, **2006**, 39, 456.
- 5 a) Paul-Roth, C. O.; Williams, J. A. G.; Letessier, J.; Simonneaux, G. *Tetrahedron Letters* **2007**, 48, 4317-4322; b) Drouet, S.; Paul-Roth, C. O.; Fattori, V.; Cocchi, M.; Williams, J. A. G. *New J. Chem.* **2011**, 35, 438-444; c) C. O. Paul-Roth, S. Drouet, A. Merhi, J. A. G. Williams, L. F. Gildea, C. Pearson, M.C. Petty, *Tetrahedron* **2013**, 69, 9625-9632.
- 6 a) Paul-Roth, C. O.; Simonneaux, G. *Tetrahedron Letters* **2006**, 47, 3275-3278; b) Paul-Roth, C. O.; Simonneaux, G. *C.R. Acad. Sci., Ser. Iib: Chim.* **2006**, 9, 1277-1286.
- 7 a) Yao, D.; Hugues, V.; Blanchard-Desce, M.; Mongin, O.; Paul-Roth, C. O.; Paul, F. *New J. Chem.* **2015**, 39, 7730-7733. (b) D. Yao, X. Zhang, O. Mongin, F. Paul, C. O. Paul-Roth, *Chem. Eur. J.*, **2016**, 22, 5583-5592.
- 8 a) Yao, D.; Hugues, V.; Blanchard-Desce, M.; Mongin, O.; Paul-Roth, C. O.; Paul, F. *Chem. Eur. J.*, **2017**, 23, 2635- 2647; b) X. Zhang, S. Ben Hassine, N. Richey, O. Mongin, M. Blanchard-Desce, F. Paul, C. O. Paul-Roth, *New J. Chem.* **2020**, 44, 4144-4157.
- 9 a) L. B. Josefsen, R. W. Boyle, *Theranostics* **2012**, 2, 916-966. b) P.-C. Lo, M. S. Rodriguez-Morgade, R. K. Pandey, D. K. P. Ng, T. Torres and F. Dumoulin, *Chem. Soc. Rev.*, **2020**, 49, 1041-1056.
- 10 See for instance: a) Z. Sun, L.-P. Zhang, F. Wu, Y. Zhao, *Adv. Funct. Mater.*, **2017**, 27, 1704079; b) F. Bolze, S. Jenni, A. Sour, V. Heitz, *Chem. Commun.*, **2017**, 53, 12857-

- 12877 and refs therein; c) M. Khurana, H. A. Collins, A. Karotki, H. L. Anderson, D. T. Cramb, B. C. Wilson, *Photochem. Photobiol.*, **2007**, *83*, 1441-1448.
- 11 a) L. Shi, C. Nguyen, M. Daurat, A. C. Dhieb, W. Smirani, M. Blanchard-Desce, M. Gary-Bobo, O. Mongin, C. Paul-Roth, F. Paul, *Chem. Commun.* **2019**, *55*, 12231-12234; b) J. Schmitt, S. Jenni, A. Sour, V. Heitz, F. Bolze, A. Pallier, C. S. Bonnet, É. Tóth and B. Ventura, *Bioconjugate Chem.*, **2018**, *29*, 3726-3738; c) J. R. Starkey, E. M. Pascucci, M. A. Drobizhev, A. Elliott and A. K. Rebane, *Biochim. Biophys. Acta*, **2013**, *1830*, 4594-4603; d) H. A. Collins, M. Khurana, E. H. Moriyama, A. Mariampillai, E. Dahlstedt, M. Balaz, M. K. Kuimova, M. Drobizhev, V. X. D. Yang, D. Phillips, A. Rebane, B. C. Wilson, H. L. Anderson, *Nat. Photonics*, **2008**, *2*, 420-424.
- 12 See for instance: a) O. Mongin, M. Sankar, M. Charlot, Y. Mir and M. Blanchard-Desce, *Tetrahedron Lett.*, **2013**, *54*, 6474-6478; b) M. A. Oar, W. R. Dichtel, J. M. Serin, J. M. J. Frechet, J. E. Roger, J.E. Slagla, P. A. Fleiz, L. S. Tan, T. Y. Ohulchanskyy, P. N. Prasad, *Chem. Mater.*, **2006**, *18*, 3682-3692. ; c) M. A. Oar, J. M. Serin, W. R. Dichtel, J. M. J. Frechet, T. Y. Ohulchanskyy, P. N. Prasad, *Chem. Mater.*, **2005**, *17*, 2267-2275.
- 13 a) J. S. Lindsey, H. C. Hsu, I. C. Schreiman, *Tetrahedron Lett.*, **1986**, *27*, 4969-5012; b) J. S. Lindsey, I. C. Schreiman, H. C. Hsu, P. C. Kearney, A. M. Marguerettaz, *J. Org. Chem.*, **1987**, *52*, 827-845.
- 14 K. Sonogashira, Y. Tohda, N. Hagihara, *Tetrahedron Lett.*, **1975**, *50*, 4467.
- 15 D. Cao, L. Zhu, Z. Liu, W. Lin *J. Photochem. Photobiol. C*, **2020**, *44*, 100371.
- 16 Xu, C.; Webb, W. W. *J. Opt. Soc. Am. B* **1996**, *13*, 481-491
- 17 Perrin, D. D.; Armarego, W. L. F. *Purification of Laboratory Chemicals*, 3rd edn., Pergamon Press, Oxford, **1988**.
- 18 Werts, M. H. V.; Nerambourg, N.; Pélégry, D.; Le Grand, Y.; Blanchard-Desce, M. *Photochem. Photobiol. Sci.* **2005**, *4*, 531-538.